5244 *Biochemistry* **2010,** *49,* 5244–5257
DOI: 10.1021/bi100391w

BIOCHEMISTRY
including biophysical chemistry & molecular biology
Article

Extensive and Varied Modifications in Histone H2B of Wild-Type and Histone Deacetylase 1 Mutant *Neurospora crassa*[†]

D. C. Anderson,*[,‡] George R. Green,[§] Kristina Smith,[‡] and Eric U. Selker[‡]

[‡]*Institute of Molecular Biology, University of Oregon, Eugene, Oregon 97403, and*
[§]*Mercer University College of Pharmacy and Health Sciences, Atlanta, Georgia 30341*

Received March 13, 2010; Revised Manuscript Received April 26, 2010

ABSTRACT: DNA methylation is deficient in a histone deacetylase 1 (HDA1) mutant (*hda-1*) strain of *Neurospora crassa* with inactivated histone deacetylase 1. Difference two-dimensional (2D) gels identified the primary histone deacetylase 1 target as histone H2B. Acetylation was identified by LC−MS/MS at five different lysines in wild-type H2B and at 11 lysines in *hda-1* H2B, suggesting *Neurospora* H2B is a complex combination of different acetylated species. Individual 2D gel spots were shifted by single lysine acetylations. FTICR MS-observed methylation ladders identify an ensemble of 20−25 or more modified forms for each 2D gel spot. Twelve different lysines or arginines were methylated in H2B from the wild type or *hda-1*; only two were in the N-terminal tail. Arginines were modified by monomethylation, dimethylation, or deimination. H2B from wild-type and *hda-1* ensembles may thus differ by acetylation at multiple sites, and by additional modifications. Combined with asymmetry-generated diversity in H2B structural states in nucleosome core particles, the extensive modifications identified here can create substantial histone-generated structural diversity in nucleosome core particles.

The lowest level of organization of eukaryotic chromosomes is achieved by wrapping ∼146 bp segments of DNA around histone octamers, which consist of a histone H3−H4 tetramer and two histone H2A−H2B dimers (*1*) . The resulting string of nucleosomes can be further condensed into higher-order assemblies. It is becoming increasingly clear that the structure of chromatin, both at the level of individual nucleosomes and at higher levels, is functionally important for genetic processes such as gene expression, recombination, DNA methylation, and DNA repair. Thus, it is of interest to define ways in which chromatin can be modified. In the past decade, a large number of enzymes have been identified that post-translationally modify histones, introducing chemical modifications, some of which are associated with gene activation and others with repression. The N-terminal tails of the individual histone subunits are prominent targets for modifications, which can alter the higher-order structure of chromatin and influence recruitment of effector molecules (*2*−*4*). Modifications can also occur within the globular histone core (*5*), affecting binding of DNA to the nucleosome lateral surface, and interactions with nucleosome remodeling complexes that control the mobility of nucleosomes on DNA (*6*).

Mass spectrometry has revolutionized the study of histones, often allowing site-specific identification of post-translational modifications such as lysine acetylation, mono-, di-, and trimethylation, arginine mono- and dimethylation, deimination, and serine and threonine phosphorylation (*7*). These and other post-translational modifications constitute the "histone code" that is important in the transmission of genetic information in cells similar to but distinct from the contributions of genes themselves (*2*, *4*). Advanced techniques such as electron transfer dissociation (*8*) and sequential ion−ion reactions (*9*) have allowed site-specific determination of modifications in highly basic regions of histones such as histone H3.

Epigenetic processes such as DNA methylation, which can result in gene silencing (*10*), have been linked to histone methylation (*11*). Patterns of aberrant DNA methylation are commonly observed in human tumors, including a global loss of DNA methylation and CpG island hypermethylation, associated with inactivation of tumor suppressor genes (*12*−*14*) and changes in expression of other genes. DNA methylation is conveniently studied in organisms that are amenable to genetic manipulation, such as *Neurospora crassa*, which has only a single gene for each core histone except H4, for which two genes have been identified (*15*). Having only a single gene for a histone subtype may facilitate association of post-translational modifications with biological phenomena. In contrast, expressed human H2B is composed of at least 11 subtypes in Jurkat cells (*16*) and 7 subtypes in Hela cells (*17*), making associations more difficult. DNA methylation is not essential in *Neurospora*, allowing study of a variety of nonlethal mutations affecting methylation. Genes involved in the control of DNA methylation in *Neurospora* include DIM-1 (*18*), the DNA methyltransferase DIM-2 (*19*), the histone H3 Lys9 methyltransferase DIM-5 (*20*), heterochromatin protein 1 [HP1 (*21*)], the histone H3 Ser10 phosphatase PP1 (*22*), and dim-7, which helps target DIM-5 to chromatin (*23*). Thus, covalent modifications of DNA and histones are involved in this process. Trichostatin A is known to block selective DNA methylation in *Neurospora* (*24*), suggesting that one or more histone deacetylases are also involved in the control of DNA methylation. Mutation of the *Neurospora* histone deacetylase

[†]This work was supported by National Institutes of Health Grant GM-35690 to E.U.S. and an Oregon Medical Research Foundation grant to D.C.A.

*To whom correspondence should be addressed. E-mail: dca0204@gmail.com. Phone: (650) 355-1168.

 Published on Web 05/12/2010

gene HDA1[1] causes a loss of DNA methylation in approximately half of all methylated regions (*25*), suggesting that analysis of the histone substrate(s) and changes in modifications associated with inactivation of this enzyme may shed light on its control of DNA methylation.

We used high-resolution 2D gels (*26*) to examine histones affected by HDA1 inactivation, identifying H2B as the most prominent HDA1 histone target in *Neurospora* (*25*). Since *Neurospora* histone modifications had not been previously characterized by mass spectrometry, we examined overall *Neurospora* H2B post-translational modifications using FTICR mass spectrometry on electroeluted H2B spots isolated from wild-type and *hda-1* strains. We then used LC−MS/MS peptide sequencing to locate modifications on specific peptides and many on specific residues. To extend the examination of post-translational modifications, results obtained using SEQUEST (*27*) were compared to modifications identified using the blind search algorithm InsPecT (*28*). Modifications were compared in H2B samples from wild-type and *hda-1* strains, and they were compared with H2B samples from other organisms. We report that *N. crassa* histone H2B can be heavily modified, including extensive methylation, diverse lysine acetylation, arginine modifications, including methylation, dimethylation, and deimination, and several likely in vitro modifications.

To examine potential function(s) of the H2B modifications, we mapped them onto the crystal structure of the *Xenopus* nucleosome core particle. The results identify modifications that may affect DNA binding in the nucleosome, as well as modifications that may alter histone subunit interactions, histone assembly, and higher-order nucleosome assemblies.

METHODS

Neurospora Cultures and Histone Purification. *N. crassa* was grown in 500 mL culture flasks in Vogel's minimal medium supplemented with 2% sucrose, 1.0 mg/mL alanine, and 1.0 mg/mL histidine at 30 °C for 24 h with shaking at 150 rpm. Mycelia were collected on Whatman filter paper and immediately frozen in liquid nitrogen. Chromatin was prepared from the frozen tissues, and histones were extracted as previously described for *Saccharomyces cerevisiae* histones, with modifications described below (*29*). The frozen tissue was ground to a fine powder using a mortar and pestle cooled with liquid nitrogen, and the powder was suspended in APB buffer [150 mM sodium chloride, 10 mM Tris-HCl, 0.5% Triton X-100, 1.0 mM phenylmethanesulfonyl fluoride, 0.2% β-mercaptoethanol, 1.0 mM sodium pervanadate, and 5.0 mM sodium fluoride (pH 8.0)]. The tissue suspension was pelleted by centrifugation at 14000*g* for 10 min. The supernatant was discarded, and the chromatin pellet was washed twice with APB buffer without 0.5% Triton X-100.

Histones were extracted from the nuclear suspensions as previously described (*26*). An equal volume of ice-cold 0.4 M H_2SO_4 was added to the nuclear suspension containing 1 mg/mL protamine sulfate in 5% acetic acid, followed by incubation on ice for 24 h, with occasional mixing. Acid-insoluble material was pelleted by centrifugation at 14000*g* for 10 min, and the supernatant was mixed with 100% TCA to a final concentration of 20% TCA and incubated on ice for 1 h to precipitate acid-soluble proteins. The precipitate was collected by centrifugation for 10 min at 14000*g* and 4 °C, and the protein pellet was resuspended in ice-cold acetone, sonicated in a bath sonicator to disperse the precipitated proteins, and recovered by centrifugation at 4 °C and 14000*g* for 10 min. The supernatant was decanted and discarded, and the acetone precipitate was air-dried at room temperature. Histones were dissolved in acetic acid/urea loading buffer (8.0 M urea, 5% acetic acid, 5% β-mercaptoethanol, and 0.2 mg/mL crystal violet) to a concentration of 5 mg/mL.

2D PAGE and Electroelution of Histones from Fixed and Stained 2D Gels. Two-dimensional AUT × AU polyacrylamide gels contained acetic acid, urea, and Triton X-100 in the horizontal dimension and acetic acid and urea in the vertical dimension and were run as described previously (*26*). The gels were stained with Coomassie blue R-250. Histone samples were purified from individual protein spots in fixed and stained polyacrylamide gels as previously described (*26*). Briefly, individual spots were excised from the gel, equilibrated in elution buffer, and eluted from the gel using a custom-made electroelution apparatus (*30*). Eluted proteins were precipitated from solution using an acetone-based ion extraction buffer to remove SDS, Coomassie blue, and other contaminants from the sample.

Proteolytic Digests of Histones. Purified histones electroeluted from 2D gel spots were dissolved in 50 mM sodium phosphate buffer (pH 7.8) with 50% trifluoroethanol or with 0.1% (w/v) acid-cleavable RapiGest detergent (Waters Corp., Milford, MA), heat-denatured at 95 °C for 20 min in a heat block, and digested for at least 12 h with a 1:10 (w/w) enzyme/substrate mixture of different proteases. Progress of the digestions was checked by MALDI-TOF mass spectrometry on an Applied Biosystems Voyager DE instrument. One protease was *Staphylococcus aureus* endoprotease gluC (Calbiochem, San Diego, CA, or Worthington Biochemical Corp., Lakewood, NJ), with digestion in 50 mM sodium phosphate buffer (pH 7.8) for at least 12 h (*31*). This pH and buffer, as well as a high enzyme:substrate ratio of 1:10 (w/w) gluC to histone H2B and relatively long digestion times, were used to enhance cleavage after aspartic acid. To enhance proteolysis at Asp residues beyond the levels seen with endoprotease gluC, other digests included 1:10 (w/w) endoprotease aspN (Roche Applied Science, Penzberg, Germany) in 50 mM sodium phosphate buffer (pH 7.8) at 37 °C for 12−24 h, or a combination of endoproteinase aspN and endoprotease gluC at pH 7.8. H2B was also digested with clostripain (Worthington Biochemical Corp.) in 100 mM sodium phosphate, 10 mM dithiothreitol, and 1 mM calcium chloride (pH 7.6). *Neurospora* H2B was not reduced and alkylated before proteolysis since it contains no cysteines. The RapiGest detergent was hydrolyzed in 0.1% formic acid before peptides were injected onto a capillary column for LC−MS/MS analysis. Peptides were analyzed with and without propionylation of the N-terminus and lysines. Propionylation, which results in peptide charge reduction and more readily interpreted MS/MS spectra, was conducted as described for histones (*32*).

LC−MS/MS Analysis of Histone H2B Peptides. Peptides were sequenced and data for identification of post-translational modifications obtained by tandem mass spectrometry on a ThermoFinnigan (San Jose, CA) LTQ-FT hybrid linear ion trap-Fourier transform ion cyclotron resonance mass spectrometer (*33*) equipped with a New Objective Inc. (Woburn, MA) PV-550 source, after

[1]Abbreviations: HDA1, histone deacetylase 1; *hda-1*, *N. crassa* strain with mutant HDA1; WT, wild-type *N. crassa*; FTICR, Fourier transform ion cyclotron resonance; MS, mass spectrometry; LC−MS/MS, liquid chromatography−tandem mass spectrometry identification of peptides; me, methyl; me2, dimethyl; me3, trimethyl; ac, acetyl; cit, citrulline; TCA, trichloroacetic acid; AUT, acetic acid/urea/Triton X-100; AU, acetic acid/urea; 2D, two-dimensional; MALDI-TOF, matrix-assisted laser desorption ionization time-of-flight; HPLC, high-performance liquid chromatography; ROC, receiver operating characteristic; SVM, support vector machine learning; NCP, nucleosome core particle.

chromatography on a 75 μm internal diameter, 5−10 cm long PicoFrit column (New Objective Inc.) self-packed with Vydac Denali C18 resin. The column was loaded with the autosampler and eluted using an Agilent nano-1100 HPLC system at a flow rate of 0.3−0.4 μL/min, with the digest eluted for 40−50 min at 5% acetonitrile and 0.1% formic acid, followed by a 3%/min increasing gradient of acetonitrile and 0.1% formic acid to 90% acetonitrile, and a 5−10 min elution at 90% acetonitrile and 0.1% formic acid. Peptide precursor ions were analyzed in the ICR cell at a resolution of 100000 and MS/MS fragments analyzed in the LTQ linear ion trap. One FT survey scan (maximum fill time of 2 s, target value of 5×10^5) triggered parallel LTQ acquisition of MS/MS spectra for the three most intense peptide ions (target value of 5×10^3, maximum fill time of 0.5 s). Monoisotopic masses were used for precursor and product ions in Bioworks Browser 3.2 SEQUEST searches, with a precursor ion mass uncertainty of 10 ppm, and a standard ion trap fragment ion mass uncertainty of 1.0 m/z. Dynamic exclusion was activated, with a maximum repetition of 2 over a 30 s time period, and an exclusion duration of 60 s. The LTQ was tuned and calibrated within 1−2 weeks of experiments, and the FT was mass-calibrated within 1−2 days of use. MS/MS spectra were plotted using Protein Prospector's MS-Product (prospector.ucsf.edu).

FTICR Mass Spectrometry. Whole-protein FTICR mass spectra of histone H2B dissolved in 50% acetonitrile and 0.1% trifluoroacetic acid were recorded using static nanospray from 4 μm tip internal diameter coated glass capillaries (New Objective Inc.), on the LTQ-FT. The instrument was mass-calibrated before use and operated at a spray voltage just above threshold, which varied for different samples and capillaries from 1.2 to 1.8 kV; data were collected at a resolution of 200000. To minimize file size, two to eight microscans were averaged for each saved scan. The histone H2B charge envelope was collected from m/z 550 to 1200 in the ICR cell. Whole protein spectra were analyzed with a commercial version of THRASH (*34*), called Xtract (ThermoFinnigan, San Jose, CA), using a 60% fit, a signal-to-noise setting of 1.3, low sulfur averagine, and a remainder of 1%.

Post-Translational Modification Analysis. SEQUEST (*27*) was used for most analyses of post-translational modifications, searching a database of 7663 protein sequences containing all *N. crassa* histone sequences, human cytokeratin sequences, sequences of the proteases used to digest electroeluted histone H2B, and reversed protein sequences of the *Nostoc punctiforme* proteome (http://genome.ornl.gov/microbial/npun/). Modification monoisotopic masses used for database searching were 42.01057 Da for acetyl, 42.04695 Da for trimethyl, 28.03130 Da for dimethyl, 14.01570 Da for methyl, 0.98402 Da for deimination, 15.99492 Da for oxidation, and 79.96633 for phosphorylation. Modification types were searched in groups of six different optional modifications. For the group of six optional modifications (without phosphorylation) described above used with the database mentioned above, the 13-parameter support vector machine learning test ROC score (*35*) from 10-fold cross validation was 0.960 ± 0.009. Numerous initial searches did not find any phosphorylated H2B sites, so further searches did not consider this modification. Modifications examined by SEQUEST included lysine (unmodified, mono-, di-, and trimethylated, and acetylated), arginine (unmodified, deiminated, and mono- and dimethylated), methionine (oxidized), and serine, threonine, and tyrosine (all phosphorylated). The precursor ion spectra of peptides identified with citrulline (Table 4), and of control peptides containing unmodified arginine, were individually examined to ensure the monoisotopic mass used in the database search was selected correctly by Bioworks Browser; a number of false positives were eliminated by this manual examination. No N-terminal H2B modifications were identified in peptides containing the N-terminus of the protein, in separate searches for mono-, di-, or trimethylation or acetylation. Peptides with termini not expected for the protease(s) used for digestion were not included in the results. The mass of a precursor ion alone, measured by FTICR-MS, is usually sufficient to derive the composition of modifications on a peptide (*36*), including distinguishing trimethyllysine from acetyllysine. The location of modifications was then derived using SEQUEST and the MS/MS spectrum, using a difference in the SEQUEST parameter delta Cn of at least 0.08 (*37*) to distinguish the top choices. In many cases, there were multiple combinations of modifications at different positions consistent with the MS and MS/MS data; thus, our set of modified sites likely underestimates the full population of modifications. Ambiguities in the site of modification are noted in the tables.

Analysis of Modifications Using InsPecT. Post-translational modifications were independently analyzed using InsPecT (*28*), version 20061212. This software did not allow a precursor ion mass tolerance in parts per million; thus, a tolerance of 0.008 Da (10 ppm mass accuracy for an 800 Da precursor) and the default product ion tolerance of 0.5 Da were used. Both one and two modifications were allowed per peptide in separate runs; the inability to analyze three or more modifications per peptide may account in part for the smaller number of modifications identified compared to SEQUEST. A maximal modification size of 95 was allowed, and the default p value cutoff was 0.05. Since cleavage after Glu and Asp or before Asp could not be specified in the program, searches requiring no enzyme specificity were used, and peptides were selected that had terminal cleavages expected for the proteases used to digest H2B. Searches allowing peptide mass modifications greater than 95 Da were difficult to interpret since extra mass was often added to peptide termini which represented extensions of the peptide sequence in H2B. The InsPecT-calculated p value reflects the probability that the match between the sequence and MS/MS spectrum is spurious; lower numbers are better. Trimethyl- and acetyllysines were manually distinguished by precursor mass accuracy after InsPecT assigned the sequence to the MS/MS spectrum.

Support Vector Machine Learning Analysis. SEQUEST results were analyzed using the support vector machine learning program GIST (*35*). Version 2.0.5 (http://microarray.cpmc.columbia.edu/gist/) was used with a quadratic kernel function, a diagonal factor of 0.03, and a constant of 10. A training set with LTQ-FT data was used for GIST analysis. Each peptide was associated with 13 parameters (*38*), including peptide-protonated mass MH, peptide charge z, peptide ion current, the difference in mass between the predicted mass of the top-ranked peptide and the experimentally observed peptide mass (dM), the SEQUEST parameters Xcorr, delta Cn, Sp, RSp, y, and b ion match (*27*), the fraction of the total MS/MS spectrum ion current matched by peaks from the best-fit peptide, the fraction of the total MS/MS spectrum peaks matched by peaks from the best-fit peptide, the total number of MS/MS spectrum peaks, and the sequence homology between the top two best-fit peptides. Probabilities of the correct sequence assignment were calculated using GIST (*35*). In the context of analysis of purified histones, and since the mass of the FTICR-MS-measured precursor ion is usually sufficient to derive the composition of modifications on a peptide

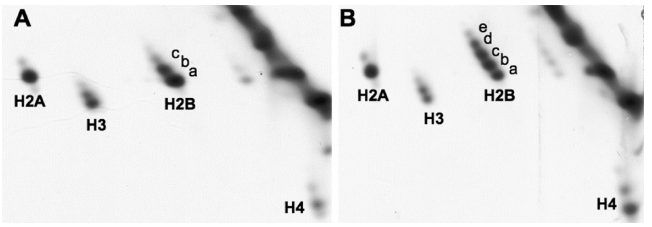

FIGURE 1: High-resolution two-dimensional polyacrylamide gel electrophoresis of histones isolated from wild-type and *hda-1* strains of *N. crassa*. Histones from wild-type (A) and *hda-1* (B) strains of *N. crassa* were resolved in acetic acid, urea, and Triton X-100 (AUT) in the horizontal dimension and acetic acid and urea (AU) in the vertical dimension. Proteins were stained with Coomassie blue R-250. All four core histones (H2A, H2B, H3, and H4) were observed. Wild-type H2B appears as a diagonal ladder of three labeled spots with a fourth faint spot, while *hda-1* H2B appears as a diagonal ladder of five spots.

(*36*), the peptide probability is useful in distinguishing the top two choices resulting from SEQUEST analysis.

RESULTS

FTICR-MS Overview of Histone H2B Modifications. We wished to characterize post-translational modifications of *Neurospora* histone H2B because our preliminary studies using AUT × AU 2D gels implicated modifications of this histone as particularly sensitive to mutation of the histone deacetylase gene *hda-1* (*25*). We used high-resolution, preparative AUT × AU 2D gels to purify acid-soluble proteins extracted from wild-type or *hda-1* lysates. The gels separate core histones H2A, H2B, H3, and H4 via the differential binding of Triton X-100 (*26*). Histone species differing by charge-altering modifications (potentially acetylation, phosphorylation, deimination, and deamidation) appear as spots trailing diagonally to the top left. Figure 1 shows a comparison of Coomassie-stained 2D gels of histones purified from wild-type (WT) and *hda-1* strains. While minor differences can be seen upon comparison of histones H4 and H3, the most pronounced differences occur with histone H2B. The diagonal ladder of spots a−e for H2B isolated from the *hda-1* strain was extended by one or two additional spots compared to the WT H2B ladder, suggesting the presence of additional modified forms of *hda-1* H2B.

To characterize differences between wild-type and *hda-1* H2B, individual H2B 2D gel spots were electroeluted from fixed and stained gels and introduced into the mass spectrometer source using static nanospray. The masses of H2B and various modified forms were obtained at high resolution (R = 200000). Figure 2 compares the FTICR mass spectrum of WT H2B spot a (the lowest spot in the H2B ladder) with the spectrum of the next higher spot in the WT H2B ladder (WT spot b), to illustrate mass shifts of similar peaks in the two spectra. No unmodified H2B, which would occur at a monoisotopic mass of 14700.97 Da, was observed. Each peak represents a carbon isotope cluster of a particular modified form (or isobaric forms). Both WT spot a and WT spot b spectra consist of approximately three clusters of approximately seven peaks, which for WT spot a are centered on peaks 3, 9, and 15 in Figure 2.

Together, ~20−25 modified forms are shown for each H2B spot, with the most highly modified forms representing a mass addition of more than 400 Da. Individual peaks in the WT spot b clusters are shifted to higher masses by 42 Da compared to corresponding peaks in the WT spot a cluster. The common shift of 42 Da suggests that most peaks in spot b have this additional

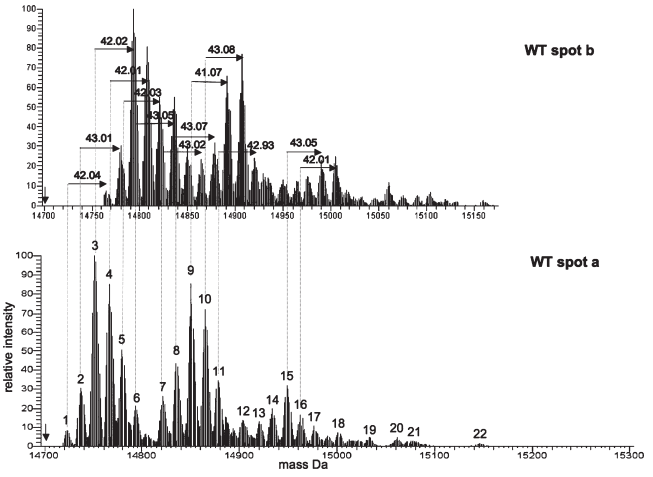

FIGURE 2: FTICR mass spectrometry of electroeluted histone H2B 2D gel spots. The monoisotopic mass of unmodified H2B is 14700.97 Da (vertical arrow). Each single spectral peak represents an isotope cluster for one or more modified forms of histone H2B. Listed mass shifts are based on monoisotopic masses calculated by THRASH (*34*), which are aligned with the most abundant isotopic peak of each isotope cluster for the sake of clarity. The spectra are aligned to allow comparison of clusters of peaks. The high-resolution mass spectrum is shown for the lowest (WT spot a) and next upper (WT spot b) wild-type histone H2B spots. Mass shifts for each peak are listed in Table 1. The *y*-axis represents relative abundance.

modification compared to peaks in spot a; the mass of 42 Da is consistent with the addition of an acetyl group. An additional modification of 1 Da in spot a (for example, from Arg conversion to citrulline, or Asn or Gln deamidation) that is not present in spot b could give rise to a shift of 41 Da, and an additional modification of 1 Da in spot b not present in spot a would give a 43 Da shift. Amounts of wild-type H2B in spot c were insufficient to allow acquisition of a good high-resolution spectrum.

Monoisotopic masses calculated for each of the major Figure 2 peaks are listed in Table 1. Most peaks are shifted from unmodified H2B by integral multiples of 14 Da or one methyl group. For each peak, the mass shifts may thus reflect the composition of methyl groups, but for some peaks, the exact composition of methylated species (mono-, di-, or trimethyllysine and/or mono- and dimethylarginine) cannot be defined from mass alone. Similar results were obtained comparing *hda-1* H2B spots a and b, with peaks in spot b shifted by +42 Da compared to peaks in spot a and with the appearance of 20−25 peaks spaced by 14 Da (see Figure 2B of the Supporting Information and the right half of Table 1). Comparison of *hda-1* H2B spots b and c gave similar results (Figure 2C of the Supporting Information), while peaks in WT spot a and *hda-1* spot a were not shifted by 42 Da when compared (Figure 2D of the Supporting Information).

LC−MS/MS Analysis of N-Terminal Peptide Methylation. To examine the location of methyl groups indicated by experiments illustrated in Figure 2, as well as the location of other modifications, electroeluted protein from all WT H2B spots (and, separately, protein from all *hda-1* spots) was combined and digested with gluC endoprotease, with a combination of aspN and gluC endoproteases, or with argC endoprotease, which can also cleave after lysine residues (*39*). Digests were then examined by capillary LC−MS/MS on an LTQ-FT instrument. Table 2 shows methylations identified on PPKPADKKPASKAPATASKAPE containing the N-terminus of H2B, and fragments of this peptide, found in wild-type and *hda-1* H2B. Some sites of lysine acetylation were also found on methylated peptides. To provide

Table 1: Mass Shifts of Monoisotopic Peaks in Histone H2B Spectra[a]

shifts in the WT spot a spectrum of Figure 2A				shifts in the *hda-1* spot a spectrum of Figure 2B			
peak	mass (Da), MH^+	shift (Da)	methyl group equivalents	peak	mass (Da), MH^+	shift (Da)	methyl group equivalents
	14701.0	0	peak not observed		14701.0	0	peak not observed
1	14715.0	14.0	1 methyl	1	14715.0	14.0	1 methyl
2	14729.1	28.1	2 methyls	2	14729.0	28.0	2 methyls
3	14743.0	42.0	3 methyls	3	14743.1	42.1	3 methyls
4	14758.1	57.1	4 methyls + 1	4	14758.1	57.1	4 methyls + 1
5	14771.1	70.1	5 methyls	5	14771.1	70.1	5 methyls
6	14785.0	84.0	6 methyls	6	14785.1	84.1	6 methyls
7	14813.1	112.1	8 methyls	7	14800.1	99.1	7 methyls + 1
8	14827.1	126.1	9 methyls	8	14812.1	111.1	8 methyls − 1
9	14842.1	141.1	10 methyls + 1	9	14827.0	126.0	9 methyls
10	14856.1	155.1	11 methyls	10	14841.1	140.1	10 methyls
11	14869.1	168.1	12 methyls	11	14856.1	155.1	11 methyls
12	14895.1	194.1	14 methyls − 3	12	14868.1	167.1	12 methyls − 2
13	14912.0	211.0	15 methyls	13	14882.1	181.1	13 methyls − 2
14	14925.1	224.1	16 methyls − 1	14	14898.0	197.0	14 methyls
15	14940.1	239.1	17 methyls	15	14911.1	210.1	15 methyls − 1
16	14954.1	253.1	18 methyls	16	14925.1	224.1	16 methyls − 1
17	14968.1	267.1	19 methyls	17	14940.1	239.1	17 methyls
18	14993.1	292.1	21 methyls − 3	18	14955.1	254.1	18 methyls + 1
19	15024.1	323.1	23 methyls	19	14994.1	293.1	21 methyls − 2
20	15052.2	351.2	25 methyls	20	15009.2	308.1	22 methyls − 1
21	15068.2	367.2	26 methyls + 2	21	15023.2	322.2	23 methyls − 1
22	15137.2	436.2	31 methyls	23	15051.1	350.1	25 methyls − 1
				24	15067.2	366.2	26 methyls + 1
				25	15107.2	406.2	29 methyls − 1
				26	15122.2	421.2	30 methyls

[a]Monoisotopic masses were calculated using THRASH (*34*). Addition of a methyl group adds 14.057 Da. Addition of an acetyl adds 42.011 Da. Arg deimination or deamidation of Asn or Gln adds 0.985 Da. The added mass from three methyls or one trimethyl, or one acetyl group probably cannot be distinguished, as the mass shift of an acetyl from a trimethyl group would be 2.47 ppm for intact H2B, which may be below the mass accuracy of these spectra.

an overall view of the extent of N-terminal modification, results are combined from the different proteolytic digestions. With use of an FTICR instrument to examine peptides, mass accuracy is sufficient to define the composition of most post-translational modifications in peptides derived from proteolytic digests of purified histones. The location in peptides of modified residues was then derived, when possible, from MS/MS spectra.

For wild-type H2B, methylated N-terminal peptides could be divided into peptides with zero, one, or two acetylated lysines. No unmodified PPKPADKKPASKAPATASKAPE was observed for either wild-type or *hda-1* H2B. Lys4 was identified separately with one, two, and three methyl groups, and Lys8 was identified with one methyl group. For this N-terminal peptide, for each acetylation state (zero, one, and two acetyls), multiple levels of methylation were observed.

For *hda-1* H2B, PPKPADKKPASKAPATASKAPE with one, two, and three acetylated Lys residues was observed, each containing one to four, two to five, and one to three methyl groups, respectively. Lys4 was identified separately with one and two methyl groups. We did not observe this peptide without an acetylated Lys, possibly because of lower relative levels of the unacetylated form of H2B (Figure 1B, spot a) than for WT H2B spot a. Often multiple different positional combinations of methyl groups, among the five lysines in this peptide, were consistent with the MS/MS spectra. Acetylation was individually identified on Lys4 (see Table 6), Lys8, Lys13, and Lys20; acetylation on Lys13 and Lys20 was identified only on multiply acetylated peptides, suggesting they may not be initial sites of acetylation in *hda-1* H2B.

LC−MS/MS Analysis of the Globular Domain and C-Terminal Lysine Methylation. Proteolytic digests of wild-type and *hda-1* H2B were examined for methylations not in the N-terminal tail, using both underivatized and propionylated H2B. Table 3 shows the identification of methylated peptides in this region. In wild-type H2B, methylated lysines included K45 or K54, K57, K97, K127, and K137 at the C-terminus. With the exception of trimethyllysine 97, modifications were methyl or dimethyl groups and occurred either alone or in combination with other Lys or Arg methyls, or citrulline. For HDA1-inactivated H2B, globular domain lysines were methylated or dimethylated at K54, K57, K90, K96, K97, and K119. Some of these occurred in combination with methylated arginine. Figure 3A shows a graphic overview of lysine methylations (and Arg modifications) in wild-type and *hda-1* H2B. The identified methylations underestimate the total methylated residues since in some cases the MS/MS spectra cannot distinguish some (particularly adjacent) methylated sites, which are not indicated in the figure. Overall, methylation appears to differ between WT and *hda-1* H2B at nine sites (Figure 3A).

LC−MS/MS Analysis of Arginine Modifications. Modifications of arginine in histones are of particular interest since arginine dimethylation may be involved in gene activation and repression, while arginine deimination to citrulline may lead to transcriptional repression (*40*). Citrulline has been observed in histones H3, H2A, and H4 (*41*) but not, to the best of our knowledge, in H2B (*42*). We thus examined different H2B peptide maps for the presence of modified arginine. LC−MS/MS analysis identified several modified arginines in both wild-type and *hda-1* H2B, listed in Table 4. In wild-type H2B, monomethylarginine was identified at R103, while dimethylarginine was identified at R110. In *hda-1* H2B, monomethylarginine was identified at R103.

Table 2: Methylation of N-Terminal Peptides of Histone H2B[a]

peptide MH^+, precursor z	PTM composition	modified sites	probability
		WT H2B	
		$PPK_4PADK_8K_9PASK_{13}$	
1277.763, 3	1 Me	K4-Me	0.86
1291.773, 4	1 Me_2	K4-Me_2	0.92
1305.800, 3	1 Me_3	K4-Me_3	0.87
		$DK_8K_9PASK_{13}APATASK_{20}APE$	
1696.922, 2	none	none	0.83
1738.981, 3	3 Me	several combinations	0.70
		$PPK_4PADK_8K_9PASK_{13}APATASK_{20}APE$	
2201.235, 3	1 Me	K4-Me	0.71
2215.242, 4	2 Me	several combinations	[b]
2215.247, 5	2 Me	K4-Me, K8-Me	0.54
2229.267, 3	1 Me_3	K4-Me_3	0.86
2257.255, 4	1Ac + 2Me	several combinations	[b]
2271.278, 4	1Ac + 3Me	multiple combinations	[b]
2285.288, 4	1Ac + 4Me	multiple combinations	[b]
2313.287, 4	2Ac + 3Me	multiple combinations	[b]
		hda-1 H2B	
		$DK_8K_9PASK_{13}APATASK_{20}APE$	
1696.939, 3	none	none	0.99
1738.962, 3	1Me_3	K8, K9, or K13	0.67
		$PPK_4PADK_8K_9PASK_{13}APATASK_{20}APE$	
2243.251, 3	1Ac + 1Me	K4-Me, K8-Ac	0.60
2257.264, 4	1Ac + 2Me	K4-Me_2, K8-Ac	0.91
2271.280, 4	1Ac + 3Me	many combinations	[b]
2285.297, 3	1Ac + 4Me	many combinations	[b]
2299.270, 3	2Ac + 2Me	most have K4-Me_2, K8-Ac	0.75
2313.296, 3	2Ac + 3Me	many combinations	[b]
2327.304, 3	2Ac + 4Me	multiple combinations	[b]
2341.323, 3	2Ac + 5Me	multiple combinations	[b]
2327.266, 3	3Ac + 1Me	three combinations	[b]
2341.286, 3	3Ac + 2Me	K4-Me_2, K20- or K13-Ac, K8- or K9-Ac	[b]
2355.300, 3	3Ac + 1Me_3	multiple combinations	[b]

[a]Residues are numbered starting with the N-terminal Met, which is removed in vivo for H2B. Site-specific modifications are indicated when uniquely identified in MS/MS spectra. The probability of correct sequencing for the top-ranked peptide is listed. In most cases, the H2B peptide and its composition of modifications are identified by mass alone. [b]Composition identified by mass.

Table 3: Histone H2B Globular Domain Lysine Methylations

peptide MH^+, precursor z	PTM composition	modified sites	probability
		WT H2B	
		$K_{45}ETYSSYIYK_{54}VLK_{57}QVHPDTGISNR$	
2826.492, 4	none	none	0.96
2854.507, 3	2Me	K45- or K54-Me_2	0.97
2854.489, 4	2Me	K57-Me_2	0.79
		$ASK_{90}LAAYNK_{96}K_{97}STISSR_{103}E$	
1853.997, 3	none	none	0.91
1882.028, 3	2Me	K96- or 97-Me_2	0.94
1896.041, 3	1Me_3	K97-Me_3	0.87
		$IQTSVRLILPGELAKHAVSEGTK_{127}AVTKYSSSTK_{137}$	
3499.969, 4	none	none	0.996
3513.980, 4	1Me	K127-Me	0.97
3527.984, 3	2Me	K127-Me_2	0.97
		$GTKAVTKYSSSTK_{137}$	
1357.733, 3	none	none	0.98
1595.859,[a] 2	1Me	K137-Me	0.81
		hda-1 H2B	
		$LAK_{119}HAVSE$	
854.472, 2	none	none	0.94
882.469, 2	2Me	K119-Me_2	0.76
		$TYSSYIYK_{54}VLK_{57}QVHPD$	
1941.009, 2	none	none	0.99
1969.012, 2	2Me	K54-Me_2	0.76
1968.988, 2	2Me	K57-Me_2	0.59
1983.100, 2	1Me_3	K57-Me_3	0.72
		$ASK_{90}LAAYNK_{96}K_{97}STISSR_{103}E$	
1854.018, 2	none	none	0.99
1882.012, 2	2Me	K90-Me_2	0.80
2064.148,[a] 2	3Me	K90-Me_2, R103-Me	0.96
2036.148,[a] 2	5Me	K96- or K97-Me_2, R103-Me	0.96
		$IQTSVRLILPGELAK_{119}HAVSE$	
2161.240, 3	none	none	0.87
2175.248, 3	1Me	K119-Me	0.98
2189.267, 3	2Me	K119-Me_2	0.94

[a]Identified after propionylation.

Our LC−MS/MS analysis did not distinguish symmetric from asymmetric arginine dimethylation.

Citrulline, which results from deimination of arginine catalyzed by peptidyl arginine deiminases (*43*−*45*), is identified by a mass gain of 0.984 Da relative to arginine. SEQUEST-identified citrulline peptide precursors were manually checked to ensure the monoisotopic peak was selected. Most of the arginines identified as modified appear to be only partially modified, as cognate unmodified peptides containing the site were also observed.

Analysis of Lysine Acetylation in Histone H2B. We used LC−MS/MS to examine differences in acetylation between H2B from WT and *hda-1* H2B. The monoisotopic masses of acetyl- and trimethyllysine differ by 0.036 Da or 18 ppm for a 2 kDa peptide; this difference in precursor ions is readily detectable using an LTQ-FT (*33*). Identified acetylated lysines not in the N-terminal tail of H2B are listed in Table 5. Lysines 96 and 97 were partially acetylated in both H2B samples. In addition, acetylated lysines were identified at positions 54, 57, and 119 of *hda-1* H2B. An MS/MS spectrum of the *hda-1* H2B peptide PPKPADKKPASKATATASKAPE identifying both dimethylation of K4 and acetylation at lysines 8 and 13 is shown in Figure 3B.

To further examine differences between WT and *hda-1* H2B, individual 2D gel spots similar to those in Figure 1 were electroeluted from two different batches of *Neurospora* in separate experiments and digested in solution with a combination of gluC and aspN endoproteases. The lowest three gel spots from both WT and *hda-1* H2B were analyzed. Results from the two separate experiments are combined in Table 6. In both experiments, numerous H2B peptides were identified (data not shown), but

Table 4: Modified Arginines in Histone H2B

peptide MH^+, precursor z	PTM composition	modified sites	probability
		WT H2B	
		$TGISR_{68}AMSILNSFVN$	
1723.881, 2	none	none	0.99
1724.864, 2	1cit[a]	R68-cit	0.69
		$ASK_{90}LAAYNKKSTISSR_{103}E$[b]	
1854.008, 2	none	none	0.88
2092.133, 2	1Me	R103-Me	0.96
2064.134, 2	3Me	R103-Me, K90-Me_2	0.90
2064.116, 2	3Me	R103-Me, K96- or 97-Me_2	0.89
2036.139, 2	5Me	R103-Me, K90-Me_2, K96- or K97-Me_2	0.88
2036.116, 2	3Me + 2Ac	R103-Me, K96- or K97-Ac, K90-Me_2	0.80
		$ASKLAAYNKKSTISSREIQTSVR_{110}LILPGE$	
3188.806, 3	2Me	R110-Me_2	0.52
		hda-1 H2B	
		$DTGISR_{68}AMSILNSFVND$	
1838.907, 2	none	none	0.90
1839.893, 2	1cit	R68-cit	0.97
		$ASKLAAYNKKSTISSR_{103}E$[b]	
1854.018, 2	none	none	0.99
2092.132, 2	1Me	R103-Me [c]	0.95

[a]cit, citrulline. [b]Identified after propionylation, except for the unmodified peptide. [c]All three top choices have R103-Me.

acetylated lysines were identified only in the N-terminal tail, in peptides DKKPASKAPATASKAPE and DAGKKTAASG. Combining both experiments, WT H2B had acetylated lysines at positions 8, 13, and 20 (and possibly position 9), while *hda-1* H2B had acetylated lysines at positions 8, 13, 20, and 29 (and possibly position 9). Generally, more acetylated sites were identified in the higher spots b and c than in spot a. Most sites were identified from peptides with one or two acetyl groups. Table 6 (bottom) summarizes additional N-terminal peptides from analyses of pooled spots in separate experiments. No additional sites of acetylated lysine were identified in WT H2B, while acetylated lysines were identified at positions 4, 8, 9, 13, and 20 for *hda-1* H2B. A summary of all of the sites of acetylation identified in WT and *hda-1* H2B is shown in Figure 3C. For spots a and b, peptides without Lys acetylation were often observed for H2B from both strains, suggesting individual H2B lysines are only partially acetylated in these spots.

For H2B isolated from both strains, no unmodified PPKPADKKPASKAPATASKAPE was identified in experiments summarized in Table 3 and in the bottom of Table 6. This explains the observation in Figure 2 that no unmodified H2B was isolated from either strain. A summary of all modifications detected by SEQUEST is shown in Figure 4B.

Analysis of Histone H2B Modifications Using the Blind Search Algorithm InsPecT. To extend the analysis of modifications in H2B, we analyzed the LC−MS/MS data using InsPecT (*28*). This algorithm searches for post-translational modifications of peptides without a prior specification of the modification mass and has been used to examine heavily modified proteins such as lens crystallins (*46*). It may thus be useful for identification of modifications not specified in the usual SEQUEST searches. To distinguish between acetyl- and trimethyllysine, the modification giving the lowest precursor mass error was selected.

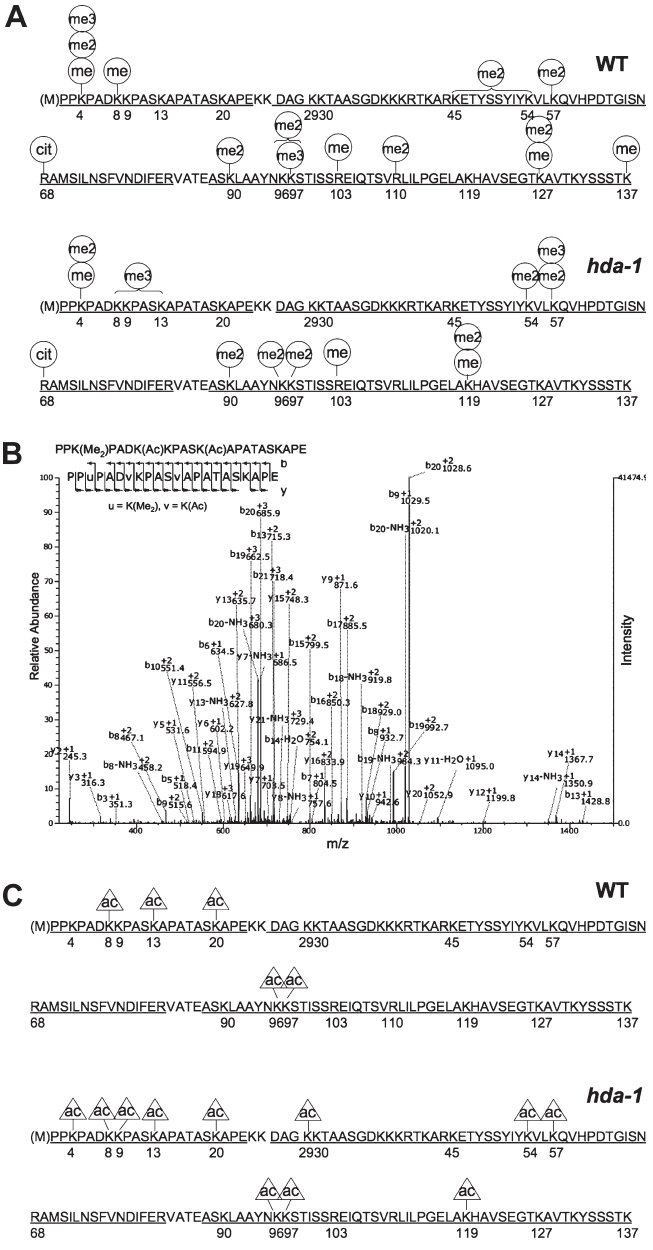

FIGURE 3: Post-translational modifications identified on *Neurospora* histone H2B. (A) Lysine and arginine modifications identified in *Neurospora* histone H2B. Modifications are indicated by circles above the modified H2B residue. The top sequence indicates modification sites in wild-type (WT) H2B; the bottom sequence shows modification sites in *hda-1* H2B. In some cases, MS/MS spectra could not distinguish which of several alternative lysines are methylated; several of these sites are indicated with brackets spanning the potential modified lysines. The sequence coverage in combined LC−MS/MS experiments is indicated by underlined residues. (B) MS/MS spectrum identifying the doubly acetylated, doubly methylated *hda-1* H2B N-terminal peptide PPK(Me_2)PADK(Ac)KPASK(Ac)APATASKAPE using SEQUEST. (C) Summary of lysine acetylation in wild-type and *hda-1* H2B. Acetylation at each of the sites is partial since other modifications (or no modification) were identified at each of the indicated sites. The sequence coverage from individual peptides is underlined. Acetylated sites in *hda-1* H2B but not in WT H2B are potential substrate sites for the HDA1 histone deacetylase.

Table 5: Non-N-Terminal Tail Acetylated Lysines in Histone H2B

peptide MH^+, precursor z	PTM composition	modified sites if identified	probability
		WT H2B	
		$ASK_{90}LAAYNK_{96}K_{97}STISSR_{103}E$	
1896.019, 3	1Ac	K97-Ac	0.92
2036.116,[a] 2	3Me + 2Ac	R103-Me, K96- or K97-Ac, K90-Me_2	0.80
		hda-1 H2B	
		$ASK_{90}LAAYNK_{96}K_{97}STISSR_{103}E$	
2036.101,[a] 2	2Ac + 3Me	K96- or K97-Ac, R103-Me, K90-Me_2	0.87
		$TYSSYIYK_{54}VLK_{57}QVHPD$	
1941.009, 2	none	none	0.99
1983.029, 2	1Ac	K57-Ac	0.72
1983.026, 2	1Ac	K54-Ac	0.68
		$LAK_{119}HAVSE$	
854.474, 2	none	none	0.93
896.483, 2	1Ac	K119-Ac	0.84

[a]Identified after propionylation.

Fewer modification sites were identified than with SEQUEST and are summarized for H2B isolated from both strains in Table 7 and Figure 4A. Some of the modifications identified by SEQUEST were also observed with InsPecT, often at the same sites, including lysine dimethylation, and lysine acetylation or trimethylation. Modifications not examined in standard SEQUEST searches, but identified by InsPecT, include methionine sulfone, asparagine and glutamine deamidation, and Glu methyl esterification.

DISCUSSION

We have performed the first detailed characterization by mass spectrometry of histone H2B from *N. crassa*, a filamentous fungus important in the history of genetics and biochemistry and a model organism useful for genetic dissection of epigenetic phenomena such as DNA methylation (*11*). High-resolution 2D acid−urea−Triton X acid−urea gels show differential modification of WT and *hda-1* H2B, identifying histone H2B as a substrate for this enzyme. Our results show *Neurospora* H2B has some novel features, and a number of modification differences between WT and *hda-1* H2B are observed. We have identified a variety of post-translational modifications, including some likely due to solution chemistry (Met oxidation and Asn and Gln deamidation), due to preparation artifacts (methyl esterification), or of unexplained origin (Met sulfone formation). Known histone modifications such as phosphorylation (*47*, *48*), ADP ribosylation (*49*), biotinylation (*50*), or methylation of the N-terminus of the histone (*51*) were not observed.

H2B Methylation. We detected no unmodified H2B. Instead, the smallest modification was a single methyl group for both WT and *hda-1* H2B. Each H2B 2D gel spot appears to represent an ensemble of 20 or more modified forms, not counting isobaric species, with many peaks spaced by 14 Da, part of apparent methylation ladders. These ladders are organized further into three or more clusters of approximately seven methylated species each. The centers of the methylation clusters are shifted by 98 Da, which could be due to addition of seven methyl groups. If the highest-mass 14 Da-shifted peaks were assigned entirely to methylation (Table 1), ca. 30 or more methyl groups could be

Table 6: Wild-Type and *hda-1* Histone H2B 2D Gel Spot Lysine Acetylations

peptide MH^+, precursor z	PTM composition	modified sites if identified	probability
		WT Spot a	
		$DK_8K_9PASK_{13}APATASK_{20}APE$	
1696.923, 2	none	none	0.99
1738.933, 3	1Ac	K8- or K9-Ac	0.78
		WT Spot b	
		$DK_8K_9PASK_{13}APATASK_{20}APE$	
1696.923, 2	none	none	0.92
1738.934, 3	1Ac	K8-Ac	0.94
		WT Spot c	
		$DK_8K_9PASK_{13}APATASK_{20}APE$	
1738.936, 3	1Ac	K8- or K9-Ac	0.86
1780.941, 2	2Ac	K13, K8- or K9-Ac	0.58
1780.957, 2	2Ac	K20, K9- or K8-Ac	0.70
		hda-1 Spot a	
		$DK_8K_9PASK_{13}APATASK_{20}APE$	
1696.921, 2	none	none	0.98
1738.933, 3	1Ac	K13-Ac	0.69
		hda-1 Spot b	
		$DK_8K_9PASK_{13}APATASK_{20}APE$	
1696.925, 2	none	none	0.99
1738.945, 3	1Ac	K8-Ac	0.87
1738.937, 2	1Ac	K13-Ac	0.61
		hda-1 Spot c	
		$DK_8K_9PASK_{13}APATASK_{20}APE$	
1738.932, 3	1Ac	K8-Ac	0.89
1738.930, 3	1Ac	K13-Ac	0.85
1780.942, 2	2Ac	K20, K8- or K9-Ac	0.57
		$DAGK_{29}K_{30}TAASG$	
947.480, 2	1Ac	K29-Ac	0.54[a]
		Pooled Spots, Multiple Experiments	
		hda-1 H2B	
		$K_8K_9PASK_{13}APATASK_{20}APE$	
1707.935, 2	3Ac	K9, K13, K20-Ac	0.88
		$PPK_4PADK_8K_9PASK_{13}APATASK_{20}APE$	
2243.251, 3	1Ac + 1Me	K8-Ac, K4-Me	0.60
2257.264, 4	1Ac + 2Me	K8-Ac, K4-Me_2	0.91
2299.270, 3	2Ac + 2Me	K13, K8-Ac, K4-Me_2	0.75
2313.290, 4	2Ac + 3Me	K4-Ac, K8-, 9-, or 13-Ac	0.86[b]

[a]Also identified by InsPecT (Table 7). [b]All top choices have K4-Ac.

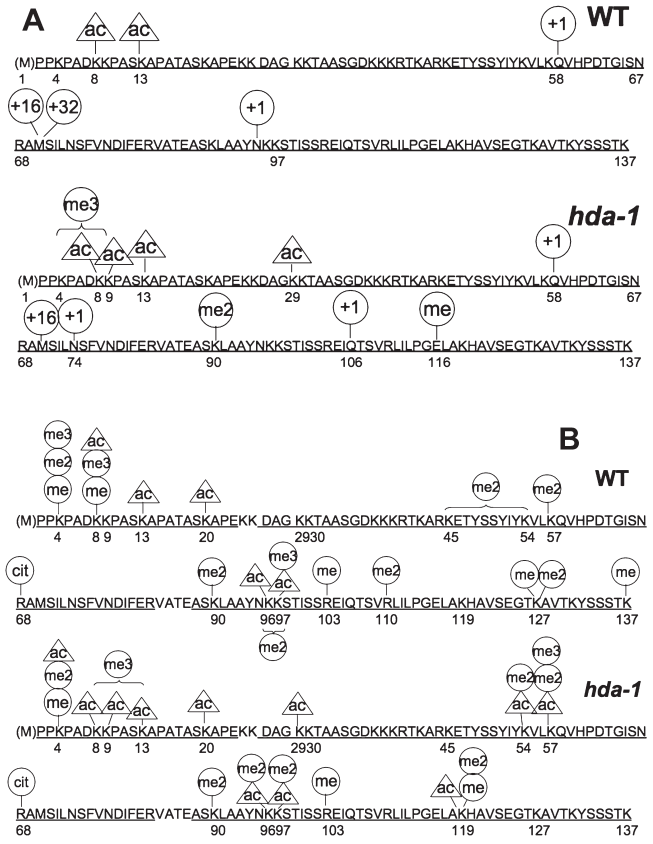

FIGURE 4: Comparison of *Neurospora* histone H2B post-translational modifications identified by two algorithms. (A) Modifications identified by the blind search algorithm InsPecT (*28*). InsPecT identified several modifications not observed in standard SEQUEST searches, including deamidated Asn or Gln (circle with +1), Met sulfone (circle with +32), and a glutamate methyl ester (me). Other modifications were oxidized Met (circle with +16), dimethyllysine (me2), trimethyllysine (me3), and acetyllysine (ac). Sequence coverage of identified peptides is indicated by underlined residues. Acetyl- and trimethyllysine were distinguished by precursor ion mass. (B) Summary of all modifications identified in wild-type and HDA1-inactivated H2B using SEQUEST, indicated by circles over modified residues: methyl (me), dimethyl (me2), trimethyl (me3), acetyl (ac), and Arg modified to citrulline (cit).

simultaneously present in a small subset of H2B molecules. By comparison with the maximal number of methyl groups identified by LC−MS/MS in Figure 3A (19 for WT H2B and 19 for *hda-1* H2B), more individual sites of methylation may remain to be identified. Since at the protein level it is more difficult to distinguish three methyls from an acetyl group, and in view of the LC−MS/MS results, some of the modified forms contain a mixture of methyl and acetyl groups. For individual gel spots, much of the heterogeneity in methylation appears to be associated with the N-terminal peptide PPKPADKKPASKAPATASKAPE, for which no unmodified species was observed. The state of methylation of this peptide explains the observation of no unmodified WT or *hda-1* H2B. Further heterogeneity in methylation is due to different methylated states of peptide ASKLAAYNKKSTISSRE. Methylated sites in H2B include mono-, di-, and trimethylated lysine, mono- and dimethylarginine, and glutamate methyl esters. Symmetric and asymmetric Arg methylation were not distinguished in these experiments. Methylation may be important as transitions among mono-, di-, and trimethyllysine may control dynamic processes such as transcription and DNA repair (*52*).

Of the 12 different sites of methylated lysine identified in WT and *hda-1* H2B, eight (Lys54, -57, -90, -96, -97, -119, -127, and -137) are not in the N-terminal tail, roughly residues 2−32 (*53*), but instead are in the globular domain of H2B. As discussed below, some of these methylated lysine residues could be involved in DNA binding or histone subunit interactions and assembly. Interestingly, Xiong et al. (*54*) detected N-terminal H2B methylation and dimethylation and confirmed our observation of mono-, di-, and trimethylation of Lys4.

Lysine Acetylation. We initially examined modifications of *Neurospora* histones for changes correlated with the absence of the HDA1 histone deacetylase. 2D gels show that the most noticeable changes in histones are in H2B, with the appearance of additional spots shifted to higher masses. Clusters of methylated H2B observed by FTICR-MS are shifted up by 42 Da in each higher gel spot, consistent with the shift being due to an additional acetylation for each higher spot. This is consistent with similar early observations from one-dimensional AUT gels (*55*, *56*) run on HPLC-isolated protein fractions. However, acetylation of H2B lysines can be complex, as we have found five different acetyllysine sites for WT H2B and 11 for *hda-1* H2B. The high ratio of different acetylated sites to the number of acetylated lysines in the 2D gel spots suggests many different individual acetylated species of H2B may exist in *Neurospora*. Approximately half of the acetylated lysine sites are in the N-terminal tail, while about half are in the globular region, where modifications may be associated with the control of dynamics of histone−DNA interactions (*6*).

In different histone preparations, different sites of acetylation were observed for WT and *hda-1* H2B, ranging from acetylation only in the N-terminal tail for the two main experiments combined in Table 6 to acetylation that includes the globular domain and closer to the C-terminus (Table 5). This range of results suggests uncontrolled variables affecting lysine acetylation, which could include differences in the physiological state of *Neurospora* cultures grown and harvested at different times, small differences in histone isolation procedures, proteolytic digestion procedures, or levels of added histone deacetylase inhibitors, or other variables. This may explain the results of Xiong et al. (*54*), who observed acetylation of WT lysines only in the N-terminal tail, at positions 8, 13, 20, 29, and 30. This variability makes identification of substrate site(s) for HDA1, expected to be lysines acetylated in *hda-1* H2B but not in WT H2B, more difficult. Current candidates include Lys4, -9, -54, -57, and/or -119. Yeast HDA1 deacetylates histone H2B as well as histone H3, with deacetylation of H2B at lysine 16, which (based on sequence alignments in Figure 5) is most homologous to *Neurospora* H2B Lys24. We cannot rule out this lysine as a substrate for HDA1 since our sequence coverage did not include residues 24 and 25. We have found that methylations at nine different sites differ between WT and *hda-1* H2B. Three of these sites (K4, K57, and K119) also differ in acetylation. The acetylation state of the substrate lysine(s) for HDA1 may be linked to the presence of modifications at other H2B sites, a possibility previously suggested (*57*).

Arginine Modifications. We have observed three modified states of arginine in *Neurospora* H2B, including monomethyl- and dimethylarginine and arginine deiminated to citrulline. Citrulline has been observed previously in histones H2A, H3, and H4 (*42*) but not, to the best of our knowledge, in H2B. Ca^{2+}-dependent peptidyl arginine deiminase 4 catalyzes arginine deimination in histones H2A, H3, and H4 in human cells (*42*) and is thought to have a broad substrate sequence specificity (*58*). By

Table 7: Analysis of Histone H2B Post-Translational Modifications Using InsPecT[a]

identified peptide	MH^+, z	p value	modification
	WT H2B		
DKKPASKAPATASKAPE	1696.924, 2	0.00143	none
DK_8+42KPASKAPATASKAPE	1738.934, 3	4.0×10^{-5}	K-Ac
DKKPASK$_{13}$+42APATASKAPE	1738.933, 3	0.0056	K-Ac
ASKLAAYNKKSTISSRE	1853.997, 3	7.0×10^{-5}	none
ASKLAAYN$_{95}$+1KKSTISSRE	1855.017, 4	0.026	N deamidation
TYSSYIYKVLKQ$_{58}$+1	1493.796, 2	0	Q deamidation before gluC cleavage
DTGISNRAMSILNSFVN	1838.905, 2	0.00035	none
DTGISNRAM$_{70}$+16SILNSFVN	1854.903, 2	2.0×10^{-5}	M oxidation
DTGISNRAM$_{70}$+32SILNSFVN	1870.900, 2	0.0069	M double oxidation
	hda-1 H2B		
PPK$_4$+42PADK$_8$+42KPASKAPATASKAPE	2271.280, 4	7.0×10^{-5}	K-Ac + K-Me$_3$[b]
DKKPASKAPATASKAPE	1696.923, 2	3.0×10^{-5}	none
DK_8+42KPASKAPATASKAPE	1738.935, 2	1.0×10^{-5}	K-Ac
DKK$_9$+42PASKAPATASKAPE	1738.931, 2	0.0006	K-Ac
DKKPASK$_{13}$+42APATASKAPE	1738.937, 3	0.0030	K-Ac
DAGK$_{29}$+42KTAASG	947.479, 2	0.00021	K-Ac
ASKLAAYNKKSTISSRE	1854.019 2	0	none
ASK$_{90}$+28LAAYNKKSTISSRE	1882.015, 2	0	K-Me$_2$
IQ$_{106}$+1TSVRLILPGELAKHAVSE	2162.220, 3	0.0263	Q deamidation
IQTSVRLILPGE$_{116}$+14LAKHAVSE	2175.255, 2	0	E methyl ester
TYSSYIYKVLKQ$_{58}$+1	1493.782, 2	0	before gluC cleavage
DTGISNRAMSILN$_{74}$+1SFVN	1839.893, 2	3.0×10^{-5}	N deamidation
TGISNRAMSILNSFVND	1838.964, 2	0	none
TGISNRAM$_{70}$+16SILNSFVND	1854.911, 2	0.0013	M oxidation

[a]Acetyl and trimethyl groups are distinguished by precursor mass. [b]Mass errors are for two acetyl groups (20.2 ppm), two trimethyl groups (11.8 ppm), or one of each (4.16 ppm).

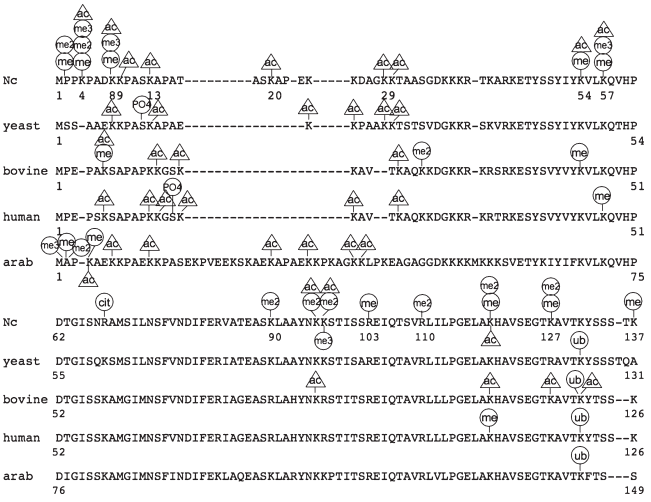

FIGURE 5: Comparison of *Neurospora* histone H2B post-translational modifications with those of histone H2B forms from other organisms. H2B sequences from *Neurospora*, yeast (*Saccharomyces cerevisiae*), calf (*Bos taurus*), *Arabidopsis* variant HTB11, and human histone H2B (locus CAB02545) were aligned using T-coffee (*59*). Numbering starts with the N-terminal Met, although this is not present in the mature histone. Modifications from wild-type and HDA1-inactivated H2B were combined for the *Neurospora* map and include three additional modifications reported by Xiong et al. (*54*).

alignment (*59*) of *Neurospora* H2B with an H2B of known structure (Table 8), all modified arginines appear to be in the globular domain of the protein rather than in the N-terminal tail. Previous sites of histone Arg deimination have been in the N-terminal tails of histones H2A, H3, and H4 (*42*, *44*); thus, the location of a site of Arg deimination in a histone globular domain may be novel. Arg methylation or dimethylation may prevent deimination by peptidyl arginine deiminases (*44*, *60*), and Arg deimination may antagonize Arg methylation. Arginine deimination to citrulline may lead to transcriptional repression (*40*). A functional interaction between Arg methylation and deimination in H2B is unclear, since at least so far, the modifications have not been found on the same arginines.

Arginine methylation may modulate intermolecular interactions, due to increased side chain bulk and loss of a hydrogen bond donor (*61*), and may be a mark for pluripotency (*62*). Histone arginine dimethylation may be involved in gene activation and repression (*40*). Three potential arginine methyltransferases, homologues of human PRMT1, -3, and -5, have been identified in the *Neurospora* genome (*63*) but, to the best of our knowledge, have not been studied in detail. Homologues of these enzymes have, however, been studied in other organisms. The homologue of PRMT1 in the fungus *Aspergillis nidulans*, RmtA, is specific for histone H4 arg3 (*64*). PRMT1-catalyzed histone asymmetric arginine dimethylation is involved in gene activation (*45*), while PRMT5 mediates symmetrical dimethylation of arginine 3 on histone H2A and/or H4 tails (*65*), which is associated with gene repression (*45*). Interestingly, arginine methylation may be indirectly linked to DNA methylation, as PRMT5 and its substrate MBD2 are recruited to CpG islands in a DNA methylation-dependent fashion in vivo, and the substrate histone H4 R3 is dimethylated at these foci (*66*). Fission yeast PRMT3 is a ribosomal protein that catalyzes the formation of asymmetric (type I) dimethylarginine (*67*), has the ribosomal protein rpS2 as a substrate in mouse cells (*68*), and is not currently known to modify histones. Thus, it is currently unclear which enzyme catalyzes monomethylation of arginine in H2B.

Table 8: Mapping of Modified *Neurospora* Histone H2B Residues onto the Structure of H2B in the *Xenopus* Nucleosome Core Particle

T-Coffee alignment of *Neurospora* and *Xenopus* histone H2B sequences

```
Nc                                                          54 57
MPPKPADKKPASKAPATASKAPEKKDAGKKTAASGDKKKRTKARKETYSSYIYKVLKQVH
xle
MP-EPAKSAPAPKKGS--------KKAVTKTQ-KKDGKKRRKTRKESYAIYVYKVLKQVH
1                                                           40 43

Nc     68                    90    9697   103    110       119
PDTGISNRAMSILNSFVNDIFERVATEASKLAAYNKKSTISSREIQTSVRLILPGELAKH
xle
PDTGISSKAMSIMNSFVNDVFERIAGEASRLAHYNKRSTITSREIQTAVRLLLPGELAKH
       54                    76    8283   89     96        105
         127
Nc  AVSEGTKAVTKYSSSTK
xle AVSEGTKAVT-YTS-AK
         113
```

Location of modified residues

N.c.	*Xenopus*	comment
K54	K40	K40 is at the top and bottom H2B surface; its N_Z is ~4.7Å to guanosine 48 01P, ~4.6Å to H2A Q24 backbone oxygen at the H2B-H2A interface
K57	K43	K43 is near the top/bottom NCP surface, ~6.7Å to thymidine 54 O1P
R68	K54	K54 is on the surface of the histone octamer but inside the DNA; N_Z is 6.7Å to guanosine 56 O1P, ~6.6Å to H3 E94 OE2
K90	R76	R76 is buried in H2B core at center of NCP, abuts small central cavity
K96	K82	K82 is on H2B surface in histone octamer but inside DNA; Nz is 7.65Å from adenosine 29 O2P
K97	R83	R83 is on surface of H2B in histone octamer but inside DNA; directly binds adenosine 33 and guanosine 34 phosphodiesters
R103	R89	R89 is at the top/bottom surface of NCP and at the H2B-H4 interface: R89 NH2 is ~3.2Å to H4 K77 N_Z, NH1 is ~2.6Å to H4 H75 carbonyl oxygen
R110	R96	R96 side chain protrudes at the top/bottom surface
K119	K105	K105 side chain protrudes from top/bottom surface
K127	K113	K113 side chain protrudes from the top/bottom surface

Mapping Modified Residues onto the Structure of Histone H2B in the Xenopus Nucleosome Core Particle. The existence of new modifications at a number of *Neurospora* H2B sites (Figure 5) raises the question of their potential function. Cosgrove et al. (*6*) proposed that single modifications of histone residues on the surface of the nucleosome modulate nucleosome dynamics by changing histone−DNA interactions and affecting DNA mobility and perhaps the exchange of histone variants into a nucleosome core particle (NCP). To examine this possibility for *Neurospora* H2B, we mapped the post-translationally modified Lys and Arg residues to residues in the highly homologous *Xenopus* H2B. Residues in the N-terminal tail were not considered because of the significant sequence differences in this region. The sequence of *Neurospora* H2B was aligned (*59*) in Table 8 with that of the *Xenopus* H2B used for the crystal structure of the NCP at 1.9 Å (*53*). There appear to be at least three classes of modified residues in *Neurospora* H2B.

Assuming (because of the high degree of sequence similarity in this region) that the globular core structure of the *Neurospora* NCP is similar to that of the *Xenopus* NCP, the location of the modified *Neurospora* H2B residues close to DNA (Figure 6A) suggests they may be involved in indirect (K54, K57, R68, and K96) or direct (K97) DNA binding. HDA1 deacetylation of acetyllysine 54 or 57 could thus tighten the binding of DNA to nucleosomes and perhaps decrease DNA mobility in NCPs. In contrast, R68 deimination to citrulline, via removal of the side chain charge, could weaken DNA−histone interactions, providing a different type of mechanism for the regulation of DNA mobility in a NCP.

A second class of locations for modified residues includes H2B Arg and Lys at or near subunit interfaces in the NCP structure. Lys54 is near the H2A−H2B interface and appears to bind directly to H2A Leu99. *Neurospora* H2B Arg103 lies at the H2B−H4 interface, where it binds to H4 His75; methylation of R103 could change H2B−H4 subunit interactions. Modification of Lys90, buried within the core of H2B, could affect the assembly and structure of H2B.

A third class of locations for modified H2B residues includes those exposed at or near the surface of the NCP, including Lys54, Lys57, Arg103, Arg110, Lys119, and Lys127 (Figure 6B). Modification of these residues could affect the binding of chromatin remodeling or other complexes or proteins to the NCP, NCP−NCP interactions, and/or formation of higher-order DNA structures. The existence of multiple modified states of surface H2B residues suggests regulation of these interactions.

Comparison with Histone H2B Forms from Other Organisms. Post-translational modifications of a number of histone H2B forms have been reported (*5*, *6*, *51*, *69*−*72*), allowing their comparison to *Neurospora* histone H2B (Figure 5; WT and *hda-1* H2B are combined). Sequences were aligned using T-coffee (*59*). New (to H2B) modifications discovered here in *Neurospora* H2B

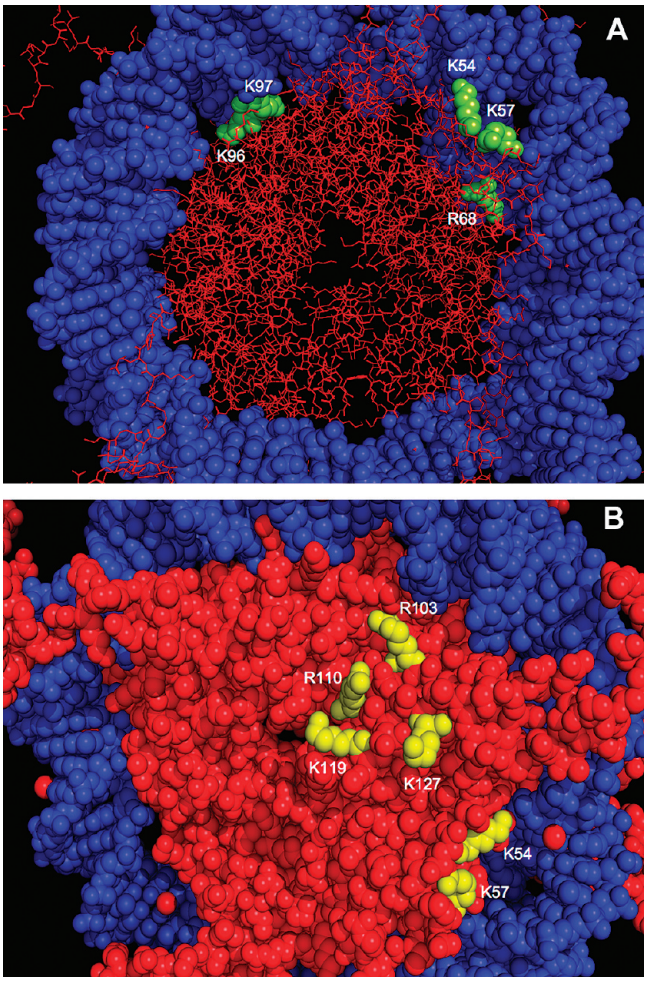

FIGURE 6: Predicted location of post-translationally modified *Neurospora* histone H2B residues in the crystal structure of the *Xenopus* nucleosome core particle. Positions of the post-translationally modified *Neurospora* H2B globular domain residues in the structure of the *Xenopus* nucleosome core particle (Protein Data Bank entry 1KX5) were derived by sequence alignment (*59*) with *Xenopus* H2B (Table 8). Residues on only one face of the nucleosome core particle structure are shown; similar residues are also on the opposite face. Histone polypeptides are colored red, modified residues yellow, and the two strands of DNA wrapped around the histone octamer blue. (A) H2B modified residues predicted to be close to DNA that may directly or indirectly bind the DNA wrapped around the core histone octamer. K96, K97, and R68 are buried in the histone octamer structure, while K54 and K57 are both at the surface of the NCP. (B) H2B residues predicted to be on or near the surface of the nucleosome core particle (NCP). Numbers are shown for *Neurospora* H2B residues.

include arginine deiminated to citrulline, Arg methylation and dimethylation, trimethyllysines, a more extensive set of modifications in the globular core, a C-terminal methyl group, and overall more extensive methylation. Included are additional modifications reported by Xiong et al. (*54*), including N-terminal methylation and dimethylation, and Lys 30 acetylation. More detailed study of the non-*Neurospora* H2B's could in the future elucidate additional modifications. A number of H2Bs are ubiquitylated near the C-terminus; we did not examine *Neurospora* H2B for this modification. Tree frog histone H2B has been reported to be unmodified (*73*). *Tetrahymena* H2B has been reported to have its N-terminal alanine mono-, di-, and trimethylated and K3 and K4 acetylated and trimethylated (*74*). Garcia et al. (*75*) have used FTICR-mass spectrometry to obtain complex envelopes of modified forms of the histone H3.2 variant from HeLa cells. However, their broadband spectrum of H2B from asynchronous HeLa S3 cells contained mainly unmodified H2B variants and a total of five isotopic clusters, suggesting far less complexity of modified forms than for H3.2 (*17*).

Trimethyllysine was identified at four different lysines in *Neurospora* H2B but, to the best of our knowledge, has not been reported in yeast, calf, human, or *Arabidopsis* histone H2B. Nine different sites of dimethyllysine were observed in *Neurospora* H2B, while only single sites were annotated in calf (*5*, *69*), human (*71*), and *Arabidopsis* H2B (*51*); none were reported in yeast H2B (*70*). After sequence alignment, novel methylation sites in *Neurospora* were seen at Lys90 and at the C-terminus at Lys137.

All of the histone H2B forms can be acetylated at a number of different sites: 11 for *Neurospora* H2B, 6 for yeast and human H2B, 8 for calf H2B, and 7 for *Arabidopsis* H2B. From the 2D gel in Figure 1 and the 42 Da mass shifts between spots, we surmise that a subpopulation of *Neurospora hda-1* H2B may have as many as five or six simultaneous acetylated lysines, or as many as three or four in WT H2B. Combined with the 11 different observed acetylation sites in *Neurospora* H2B, many combinations of individual acetylated species of *Neurospora* H2B are possible. Other organisms can generate H2B sequence variants using multiple genes. Possessing only a single histone H2B gene, *Neurospora* may achieve high effective sequence diversity with a more extensive use of post-translational modifications. The N-terminal H2B tails are asymmetric in the *Xenopus* NCP crystal structure (*53*), with one tail extending into solution and the second binding between the two strands of DNA wrapped around the histone octamer, creating (with multiple N-terminal tail modifications) a mechanism for generation of even more diversity at the structural level. Given the different structures of the two NCP H2B N-terminal tails, it is possible that modifications in one tail are different from those in the other tail in a single NCP, creating an even greater diversity of NCP structural states. Further diversity could be created by differing DNA sequences bound in individual NCPs.

Other Modifications. Met59 and Met62 of human H2B isolated from nickel-treated cells have been observed as sulfoxides, and a single deamidated Gln was also observed (*76*). The in vivo significance of Met oxidation to Met sulfoxide is unclear, since this can occur in solution as well as in vivo (*77*). Identification of Met sulfone in a histone peptide is unexpected since this should require prior exposure to a strong oxidizing agent. The in vivo significance of methyl esterification and deamidation is also unclear. The 2D gels were destained in methanol, and glutamate methyl esterification has been observed when gels are stained with Coomassie blue in the presence of acid and methanol (*78*). Deamidation of both Asn and Gln can occur spontaneously in solution (*79*). An algorithm capable of simultaneously searching a large number of different modifications on a peptide, as well as allowing the presence of multiple simultaneous modifications, will be advantageous for more in-depth analysis of highly modified histone peptides.

ACKNOWLEDGMENT

We thank Stephen Tanner (University of California at San Diego, La Jolla, CA) for advice on the use of InsPecT and for a number of requested bug fixes.

SUPPORTING INFORMATION AVAILABLE

High-resolution FTMS spectra comparing methylation of *hda-1* spots a and b (Figure 2B), *hda-1* spots b and c (Figure 2C), and

WT spot a and *hda-1* spot a (Figure 2D) and annotated MS/MS spectra for peptides identified in Tables 2−7. This material is available free of charge via the Internet at http://pubs.acs.org.

REFERENCES

1. McGhee, J. D., and Felsenfeld, G. (1980) Nucleosome structure. *Annu. Rev. Biochem. 49*, 1115–1156.
2. Strahl, B., and Allis, C. (2000) The language of covalent histone modifications. *Nature 403*, 41–45.
3. Green, G. R. (2001) Phosphorylation of histone variant regions in chromatin: Unlocking the linker? *Biochem. Cell Biol. 79*, 275–287.
4. Fischle, W., Wang, Y., and Allis, C. D. (2003) Binary switches and modification cassettes in histone biology and beyond. *Nature 425*, 475–479.
5. Zhang, L., Eugeni, E., Parthun, M. R., and Freitas, M. (2003) Identification of novel histone post-translational modifications by peptide mass fingerprinting. *Chromosoma 112*, 77–86.
6. Cosgrove, M., Boeke, J., and Wolberger, C. (2004) Regulated nucleosome mobility and the histone code. *Nat. Struct. Mol. Biol. 11*, 1037–1043.
7. Garcia, B., Shabanowitz, J., and Hunt, D. (2007) Characterization of histones and their post-translational modifications by mass spectrometry. *Curr. Opin. Chem. Biol. 11*, 66–73.
8. Mikesh, L., Ueberheide, B., Chi, A., Coon, J., Syka, J., Shabanowitz, J., and Hunt, D. (2006) The utility of ETD mass spectrometry in proteomic analysis. *Biochim. Biophys. Acta 1764*, 1811–1822.
9. Coon, J., Ueberheide, B., Syka, J., Dryhurst, D., Ausio, J., Shabanowitz, J., and Hunt, D. (2005) Protein identification using sequential ion/ion reactions and tandem mass spectrometry. *Proc. Natl. Acad. Sci. U.S.A. 102*, 9463–9468.
10. Richards, E., and Elgin, S. (2002) Epigenetic Codes for Heterochromatin Formation and Silencing: Rounding up the Usual Suspects. *Cell 108*, 489–500.
11. Freitag, M., and Selker, E. (2005) Controlling DNA methylation: Many roads to one modification. *Curr. Opin. Genet. Dev. 15*, 191–199.
12. Jones, P. (2002) DNA methylation and cancer. *Oncogene 21*, 5358–5360.
13. Esteller, M. (2005) DNA methylation and cancer therapy: New developments and expectations. *Curr. Opin. Oncol. 17*, 55–60.
14. Szyf, M., Pakneshan, P., and Rabbani, S. (2004) DNA demethylation and cancer. *Cancer Lett. 211*, 133–143.
15. Hays, S., Swanson, J., and Selker, E. (2001) Identification and Characterization of the Genes Encoding the Core Histones and Histone Variants of *Neurospora crassa*. *Genetics 160*, 961–973.
16. Bonenfant, D., Coulot, M., Towbin, H., Schindler, P., and van Oostrum, J. (2006) Characterization of histone H2A and H2B variants and their post-translational modifications by mass spectrometry. *Mol. Cell. Proteomics 5*, 541–552.
17. Siuti, N., Roth, M., Mizzen, C., Kelleher, N., and Pesavento, J. (2006) Gene-specific characterization of human histone H2B by electron capture dissociation. *J. Proteome Res. 5*, 233–239.
18. Foss, H., Roberts, C., and Selker, E. U. (1998) Mutations in the dim-1 gene of *Neurospora crassa* reduce the level of DNA methylation. *Mol. Gen. Genet. 259*, 60–71.
19. Kouzminova, E., and Selker, E. U. (2001) dim-2 encodes a DNA methyltransferase responsible for all known cytosine methylation in *Neurospora*. *EMBO J. 20*, 4309–4323.
20. Tamaru, H., and Selker, E. U. (2001) A histone H3 methyltransferase controls DNA methylation in *Neurospora crassa*. *Nature 414*, 277–283.
21. Freitag, M., Hickey, P., Khlafallah, T., Read, N., and Selker, E. (2004) HP1 is essential for DNA methylation in *Neurospora*. *Mol. Cell 13*, 427–434.
22. Adhvaryu, K. K., and Selker, E. U. (2008) Protein phosphatase PP1 is required for normal DNA methylation in Neurospora. *Genes Dev. 22*, 3391–3396.
23. Lewis, Z., Adhvaryu, K., Honda, S., Shriver, A., and Selker, E. U. (2010) Identification of DIM-7, a protein required to target the DIM-5 H3 methyltransferase to chromatin. *Proc. Natl. Acad. Sci. U.S.A. 107*, 8310–8315.
24. Selker, E. U. (1998) Trichostatin A causes selective loss of DNA methylation in *Neurospora*. *Proc. Natl. Acad. Sci. U.S.A. 95*, 9430–9435.
25. Smith, K., Dobosy, J., Do, D., Riefsnyder, J., Anderson, D., Green, G., and Selker, E. (2010) manuscript in preparation.
26. Green, G. R., and Do, D. P. (2008) Purification and analysis of variant and modified histones using 2D PAGE. *Methods Mol. Biol. 464*, 285–302.
27. Eng, J., McCormack, A., and Yates, J. (1994) An approach to correlate tandem mass spectral data of peptides with amino acid sequences in a protein database. *J. Am. Soc. Mass Spectrom. 5*, 976–989.
28. Tanner, S., Shu, H., Frank, A., Wang, L., Zandi, E., Mumby, M., Pevzner, P., and Bafna, V. (2005) InsPecT: Identification of Post-translationally Modified Peptides from Tandem Mass Spectra. *Anal. Chem. 77*, 4626–4639.
29. Wyatt, H., Liaw, H., Green, G. R., and Lustig, A. J. (2003) Multiple roles for *Saccharomyces cerevisiae* histone H2A in telomere position effect, *spt* S sppression and DSB repair. *Genetics 164*, 47–64.
30. Green, G. R., Poccia, D. L., and Herlands, L. (1982) A multisample device for electroelution, concentration and dialysis of proteins from fixed and stained gel slices. *Anal. Biochem. 123*, 66–73.
31. Sorensen, S., Sorensen, T., and Breddam, K. (1991) Fragmentation of proteins by *S. aureus* strain V8 protease. *FEBS Lett. 294*, 195–197.
32. Garcia, B., Busby, S., Shabanowitz, J., Hunt, D., and Mishra, N. (2005) Resetting the epigenetic histone code in the MRL-lpr/lpr mouse model of lupus by histone deacetylase inhibition. *J. Proteome Res. 4*, 2032–2042.
33. Syka, J., Marto, J., Bai, D., Horning, S., Senko, M., Schwartz, J., Ueberheide, B., Garcia, B., Busby, S., Muratore, T., Shabanowitz, J., and Hunt, D. (2004) Novel linear quadrupole ion trap/FT mass spectrometer: Performance characterization and use in the comparative analysis of histone H3 post-translational modifications. *J. Proteome Res. 3*, 621–626.
34. Horn, D., Zubarev, R., and McLafferty, F. (2000) Automated reduction and interpretation of high resolution electrospray mass spectra of large molecules. *J. Am. Soc. Mass Spectrom. 11*, 320–332.
35. Pavlidis, P., Wapinski, I., and Noble, W. (2004) Support vector machine classification on the web. *Bioinformatics 20*, 586–587.
36. Freitas, M., Sklenar, A., and Parthun, M. (2004) Application of mass spectrometry to the identification and quantification of histone post-translational modifications. *J. Cell. Biochem. 92*, 691–700.
37. Washburn, M., Wolters, D., and Yates, J. (2001) Large-scale analysis of the yeast proteome by multidimensional protein identification technology. *Nat. Biotechnol. 19*, 242–247.
38. Anderson, D., Li, W., Payan, D., and Noble, W. (2003) A new algorithm for the evaluation of shotgun peptide sequencing in proteomics: Support vector machine classification of peptide MS/MS spectra and SEQUEST scores. *J. Proteome Res. 2*, 137–146.
39. Mitchell, W., and Harrington, W. (1968) Purification and properties of clostridiopeptidase B (clostripain). *J. Biol. Chem. 243*, 4683–4692.
40. Wysocka, J., Allis, C., and Coonrod, S. (2006) Histone arginine methylation and its dynamic regulation. *Front. Biosci. 11*, 344–355.
41. Nakashima, K., Hagiwara, T., and Yamada, M. (2002) Nuclear localization of peptidylarginine deiminase V and histone deimination in granulocytes. *J. Biol. Chem. 277*, 49562–49568.
42. Hagiwara, T., Hidaka, Y., and Yamada, M. (2005) Deimination of histone H2A and H4 at arginine 3 in HL-60 granulocytes. *Biochemistry 44*, 5827–5834.
43. Fujisaki, M., and Sugawara, K. (1981) Properties of peptidylarginine deiminase from the epidermis of newborn rats. *J. Biochem. 89*, 257–263.
44. Cuthbert, G., Daujat, S., Snowden, A., Erdjument-Bromage, H., Hagiwara, T., Yamada, M., Schneider, R., Gregory, P., Tempst, P., Bannister, A., and Kouzarides, T. (2004) Histone deimination antagonizes arginine methylation. *Cell 118*, 545–553.
45. Thompson, P., and Fast, W. (2006) Histone citrullination by protein arginine deiminase: Is arginine methylation a green light or a roadblock? *ACS Chem. Biol. 1*, 433–441.
46. Wilmarth, P., Tanner, S., Dasari, S., Nagalla, S., Riviere, M., Bafna, V., Pevzner, P., and David, L. (2006) Age-related changes in human crystallins determined from comparative analysis of post-translational modifications in young and aged lens: Does deamidation contribute to crystallin insolubility? *J. Proteome Res. 5*, 2554–2566.
47. Ajiro, K. (2000) Histone H2B phosphorylation in mammalian apoptotic cells. An association with DNA fragmentation. *J. Biol. Chem. 275*, 439–443.
48. Cheung, W., Ajiro, K., Samejima, K., Kloc, M., Cheung, P., Mizzen, C., Beeser, A., Etkin, L., Chernoff, J., Earnshaw, W., and Allis, C. D. (2003) Apoptotic phosphorylation of histone H2B is mediated by mammalian sterile twenty kinase. *Cell 113*, 507–517.
49. Burzio, L., Riquelme, P., and Koide, S. (1979) ADP ribosylation of rat liver nucleosomal core histones. *J. Biol. Chem. 254*, 3029–3037.
50. Hassan, Y., and Zempleni, J. (2006) Epigenetic regulation of chromatin structure and gene function by biotin. *J. Nutr. 136*, 1763–1765.
51. Bergmüller, E., Gehrig, P., and Gruissem, W. (2007) Characterization of post-translational modifications of histone H2B-variants isolated from *Arabidopsis thaliana*. *J. Proteome Res. 6*, 3655–3668.

52. Shahbazian, M., Zhang, K., and Grunstein, M. (2005) Histone H2B ubiquitylation controls processive methylation but not monomethylation by Dot1 and Set1. *Mol. Cell 19*, 271–277.
53. Davey, C., Sargent, D., Luger, K., Maeder, A., and Richmond, T. (2002) Solvent mediated interactions in the structure of the nucleosome core particle at 1.9 Å resolution. *J. Mol. Biol. 319*, 1097–1113.
54. Xiong, L., Adhvaryu, K., Selker, E. U., and Wang, Y. (2010) Mapping of Lysine Methylation and Acetylation in Core Histones of *Neurospora crassa*. *Biochemistry* DOI 10.1021/bi1001322.
55. Waterborg, J., Robertson, A., Tatar, D., Borza, C., and Davie, J. (1995) Histones of *Chlamydomonas reinhardtii*. Synthesis, acetylation and methylation. *Plant Physiol. 109*, 393–407.
56. Waterborg, J. (2000) Steady-state Levels of Histone Acetylation in *Saccharomyces cerevisiae*. *J. Biol. Chem. 275*, 13007–13011.
57. Robyr, D., Suka, Y., Xenarios, I., Kurdistani, S. K., Wang, A., Suka, N., and Grunstein, M. (2002) Microarray deacetylation maps determine genome-wide functions for yeast histone deacetylases. *Cell 109*, 437–446.
58. Arita, K., Shimizu, T., Hashimoto, H., Hidaka, Y., Yamada, M., and Sato, M. (2006) Structural basis for histone N-terminal recognition by human peptidylarginine deiminase 4. *Proc. Natl. Acad. Sci. U.S.A. 103*, 5291–5296.
59. Notredame, C., Higgins, D., and Heringa, J. (2000) T-Coffee: A novel method for fast and accurate multiple sequence alignment. *J. Mol. Biol. 302*, 205–217.
60. Raijmakers, R., Zendman, A. J., Egberts, W., Vossenaar, E., Raats, J., Soede-Huijbregts, C., Rutjes, F., van Veelen, P., Drijfhout, J., and Pruijn, G. (2007) Methylation of arginine residues interferes with citrullination by peptidylarginine deiminases in vitro. *J. Mol. Biol. 367*, 1118–1129.
61. McBride, A., and Silver, P. (2001) State of the arg: Protein methylation at arginine comes of age. *Cell 106*, 5–8.
62. Torres-Padilla, M., Parfitt, D., Kouzarides, T., and Zernicka-Goetz, M. (2007) Histone arginine methylation regulates pluripotency in the early mouse embryo. *Nature 445*, 214–218.
63. Borkovich, K.; et al. (2004) Lessons from the Genome Sequence of *Neurospora crassa*: Tracing the Path from Genomic Blueprint to Multicellular Organism. *Microbiol. Mol. Biol. Rev. 68*, 1–108.
64. Trojer, P., Dangl, M., Bauer, I., Graessle, S., Loidl, P., and Brosch, G. (2004) Histone methyltransferases in *Aspergillus nidulans*: Evidence for a novel enzyme with a unique substrate specificity. *Biochemistry 43*, 10834–10843.
65. Ancelin, K., Lange, U., Hajkova, P., Schneider, R., Bannister, A. J., Kouzarides, T., and Surani, M. (2006) Blimp1 associates with Prmt5 and directs histone arginine methylation in mouse germ cells. *Nat. Cell Biol. 8*, 623–630.
66. Le Guezennec, X., Vermeulen, M., Brinkman, A., Hoeijmakers, W., Cohen, A., Lasonder, E., and Stunnenberg, H. (2006) MBD2/NuRD and MBD3/NuRD, two distinct complexes with different biochemical and functional properties. *Mol. Cell. Biol. 26*, 843–851.
67. Bachand, F., and Silver, P. (2004) PRMT3 is a ribosomal protein methyltransferase that affects the cellular levels of ribosomal subunits. *EMBO J. 23*, 2641–2650.
68. Swiercz, R., Cheng, D., Kim, D., and Bedford, M. (2007) Ribosomal protein rpS2 is hypomethylated in PRMT3-deficient mice. *J. Biol. Chem. 282*, 16917–16923.
69. Thorne, A., Sautiere, P., Briand, G., and Crane-Robinson, C. (1987) The structure of ubiquitinated histone H2B. *EMBO J. 6*, 1005–1010.
70. Parra, M., Kerr, D., Fahy, D., Pouchnik, D., and Wyrick, J. (2006) Deciphering the roles of the histone H2B N-terminal domain in genome-wide transcription. *Mol. Cell. Biol. 26*, 3842–3852.
71. Beck, H. C., Nielsen, E., Matthiesen, R., Jensen, L., Sehested, M., Finn, P., Grauslund, M., Hansen, A., and Jensen, O. (2006) Quantitative proteomic analysis of post-translational modifications of human histones. *Mol. Cell. Proteomics 5*, 1314–1325.
72. Ahn, S., Diaz, R., Grunstein, M., and Allis, C. (2006) Histone H2B deacetylation at lysine 11 is required for yeast apoptosis induced by phosphorylation of H2B at serine 10. *Mol. Cell 24*, 211–220.
73. Kawasaki, H., Isaacson, T., Iwamuro, S., and Conlon, J. (2003) A protein with antimicrobial activity in the skin of Schlegel's green tree frog *Rhacophorus schlegelii* (Rhacophoridae) identified as histone H2B. *Biochem. Biophys. Res. Commun. 312*, 1082–1086.
74. Medzihradszky, K., Zhang, X., Chalkley, R. J., Guan, S., McFarland, M. A., Chalmers, M. J., Marshall, A. G., Diaz, R. L., Allis, C. D., and Burlingame, A. L. (2004) Characterization of *Tetrahymena* Histone H2B Variants and Posttranslational Populations by Electron Capture Dissociation (ECD) Fourier Transform Ion Cyclotron Mass Spectrometry (FT-ICR MS). *Mol. Cell. Proteomics 3*, 872–876.
75. Garcia, B., Pesavento, J., Mizzen, C., and Kelleher, N. (2007) Pervasive combinatorial modification of histone H3 in human cells. *Nat. Methods 4*, 487–489.
76. Karaczyn, A., Golebiowski, F., and Kasprzak, K. (2005) Truncation, deamidation, and oxidation of histone H2B in cells cultured with nickel(II). *Chem. Res. Toxicol. 18*, 1934–1942.
77. Hoshi, T., and Heinemann, S. (2001) Regulation of cell function by methionine oxidation and reduction. *J. Physiol. 531*, 1–11.
78. Haebel, S., Albrecht, T., Sparbier, K., Walden, P., Komer, R., and Steup, M. (1998) Electrophoresis-related protein modification: Alkylation of carboxy residues revealed by mass spectrometry. *Electrophoresis 19*, 679–686.
79. Peters, B., and Trout, B. (2006) Asparagine deamidation: pH-dependent mechanism from density functional theory. *Biochemistry 45*, 5384–5392.